Nanoscale

Accepted Manuscript

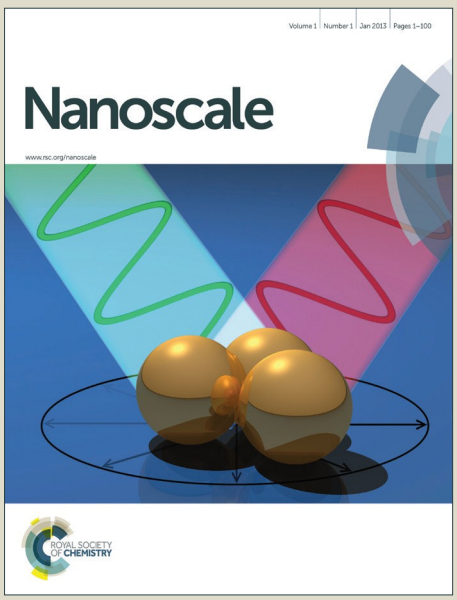

ROYAL SOCIETY OF CHEMISTRY

www.rsc.org/nanoscale

LOCALIZATION OF ADHESINS IN THE SURFACE OF PATHOGENIC BACTERIAL ENVELOPE THROUGH ATOMIC FORCE MICROSCOPY

L. Arnal[1], G. Longo[2], P. Stupar[2], M.F. Castez[3], N. Cattelan[1], R.C. Salvarezza[3], O.M. Yantorno[1], S. Kasas[2,*] and M.E. Vela[3,*]

[1] Centro de Investigación y Desarrollo de Fermentaciones Industriales (CINDEFI-CONICET-CCT La Plata), Facultad de Ciencias Exactas, UNLP. 50 N^0 227; 1900 La Plata, Argentina.

[2] Laboratory of Physics of Living Matter, Institute of Physics of Biological Systems, School of Basic Sciences, EPFL, 1015 Lausanne, Switzerland

[3] Instituto de Investigaciones Fisicoquímicas Teóricas y Aplicadas (INIFTA), Universidad Nacional de La Plata – CONICET, Sucursal 4 Casilla de Correo 16; 1900 La Plata, Argentina.

ABSTRACT

Bacterial adhesion is the first and a significant step in establishing infection. This adhesion normally occurs in presence of flow of fluids. Therefore, bacterial adhesins must be able to provide high strength interactions with their target surface in order to maintain the adhered bacteria under hydromechanical stressing conditions. In the case of *B. pertussis*, a Gram-negative bacterium responsible of pertussis, a highly contagious human respiratory tract infection, an important protein participating in the adhesion process is a 220 KDa adhesin named Filamentous haemagglutinin (FHA), an outer membrane and also secreted protein that contains recognition domains to adhere to ciliated respiratory epithelial cells and macrophages. In this work, we obtained information of the cell-surface localization and distribution of the *B. pertussis* adhesin FHA using an antibody-functionalized AFM tip. Through the analysis of specific molecular recognition events we built a map of the spatial distribution of the adhesin which revealed a non-homogenous pattern. Moreover, our experiments showed a force induced reorganization of the adhesin in the surface of the cells, which could explain a reinforced adhesive response under external forces. This single-molecule information contributes to the understanding of basic molecular mechanisms used by bacterial pathogens to cause infectious disease and to gain insight into the structural features by which adhesins can act as force sensors under mechanical shear conditions.

**** Corresponding authors:***

- M.E. Vela. E-mail: mevela@inifta.unlp.edu.ar, http://nano.quimica.unlp.edu.ar/

TEL : +54 221 4257430. FAX : +54 221 4254642.

- S.Kasas. E-mail: sandor.kasas@epfl.ch

TEL/FAX: +41 21 693 04 22. http://lpmv.epfl.ch/

Keywords : bacteria, biofilms, Force spectroscopy, Molecular recognition, adhesins.

1. Introduction

Whooping cough or pertussis is a highly contagious human respiratory tract infection caused principally by the Gram-negative bacterium *Bordetella pertussis.* Despite sustained high vaccination coverage worldwide since 1950´s, the disease remains endemic with infections peaks every 3-5 years. [1, 2] Interestingly, in the last two decades the reported cases of pertussis have been increased in several countries and changes in the age of the affected patients, from young children of less than 6 month to adolescents and adults, were reported. A decrease in acellular vaccines effectiveness and pathogen adaptation to the immunity conferred by vaccines has been suggested as possible causes for pertussis reemergence. This new scenario implies the bacterial persistence in vaccinated population and represents a risk of contagion for non-vaccinated children. A possible explanation for the continued persistence of pertussis in the community could be associated to the ability showed by *Bordetella spp* to form biofilm in the upper respiratory tract of infected animals. [3-5] The successful establishment of a biofilm community relies strongly in the adhesion step to the surface; which is mediated by different adhesins exposed in the cell surface that irreversibly interacts with the substrate. [6] Bacterial adhesion is the first and a significant step in establishing infection. In the course of colonization, adhered bacteria have to resist shear forces that act as natural defense to remove them. Therefore, bacterial adhesins must prove strength interactions with their target cells in order to maintain the adhered bacteria under these hydromechanical stressing conditions. Protein and non-protein factors have been shown to function as adhesins and promote biofilm formation in *Bordetella pertussis*.[7] In the case of proteins, they interact with different components of the respiratory epithelium to allow the attachment of the cells. Among them, the most studied proteins are Pertactine, a 69KDa autotransporter adhesin[8]; Fimbriae, which is a filamentous protein[8]; and a 220 KDa adhesin named Filamentous haemagglutinin (FHA). The latter is a lineal filamentous protein belonging to the b-selenoid family, found on the outer membrane, but also secreted. FHA contains recognition domains to adhere to ciliated respiratory epithelial cells and macrophages, and two domains composed of tandem repeat motifs.[9-11] FHA has been demonstrated to participate not only in the first adhesion step during biofilm development but has also been proved to participate in cell-cell interactions to generate the definitive structure of mature biofilm *in vitro.* Thus, the study of the spatial organization under specific recognition forces should contribute to understand the role of FHA in the adhesion step of biofilm formation.[5 12]

The studies of the presence and distribution of adhesins on cell-surface are essential to understand the adhesion capacity of a particular bacterium in the first steps of pathogenesis. In this aspect, the atomic force microscopy (AFM) constitutes a powerful technique not only by its capability to explore the surface heterogeneity of the cell envelope with nanometer resolution, but also because it allows the possibility of mapping the distribution of particular molecules of the cell surface. Such maps are obtained using the specificity of ligand-receptor interactions in experiments performed in physiological conditions, using functionalized AFM tips.[13-17] In particular, the role of the spatial organization of surface adhesins has been explored by single-molecule AFM experiments[18-20].

In this work, using atomic force microscopy we obtained information of the cell-surface localization and distribution of *B. pertussis* adhesin-FHA. The quantitative evaluation of the adhesion forces between FHA placed on the cell surface of *B. pertussis* and a specific antibody-functionalized AFM tip was employed to this aim. We made use of this information to build a map of the spatial distribution of the adhesin which revealed a non-homogenous pattern. Moreover, our experiments showed a force induced reorganization of the adhesin in the surface of the cells, which could explain a reinforced adhesive response under external forces. This single-molecule information contributes to the understanding of basic molecular mechanisms used by bacterial pathogens to cause infectious disease and to gain insight into the structural features by which adhesins can act as force sensors under mechanical shear conditions.

2. Materials and Methods

2.1. Bacterial Strains and Growth Conditions

B. pertussis Tohama I, a wild-type strain (8132 collection of Pasteur Institute, Paris, France) and *B. pertussis* GR4, a Tohama I derivative mutant lacking the expression of FHA (FHA-)[21], were used throughout this study. Stock cultures were grown on Bordet-Gengou agar (BGA; Difco Laboratories, Detroit, USA) plates supplemented with 1% w/v Bactopeptone (Difco) and 15% v/v defibrinated sheep blood (Instituto Biológico, La Plata, Argentina) at 37°C for 72h, and then subcultured for 48h in the same conditions. In the case of the FHA- strain, 50 μg ml^{-1} streptomycin (Sigma, St. Louis, MO, USA) were added to the culture media to maintain restrictive conditions. Liquid cultures were performed by inoculating bacteria into 100 ml Erlenmeyer flasks containing 30 ml of Stainer-Scholte (SS) broth, adjusting the optical density at 650 nm (OD_{650}) to 0.20 and incubating the flasks at

37ºC under shaking conditions (160 rpm). Cells of the two strains were harvested at middle-exponential phase (centrifugation at 8000*g* for 5 min) and washed twice with Phosphate Buffered Saline (PBS) buffer.

2.2. AFM measurements

2.2.i Sample Preparation

Bacteria were electrostatically-immobilized onto polyethylenimine (PEI) pre-coated glass slides (Sigma) according to previous protocols.[22, 23] Briefly, glass slides were washed twice with 96% (v/v) ethanol and Milli-Q water and then incubated overnight at 4°C with 0.1% (w/v) aqueous PEI solution. After the incubation, PEI-coated slides were rinsed twice with Milli-Q water. Bacteria were immobilized by depositing 50 µl of bacterial suspension at an OD_{650} of 1.0 over the PEI-coated slides and they were let to attach to the substrate for 2.5 h. Afterward, the slides were washed three times with distillated water to remove non adhered cells before AFM imaging.

Purified FHA (NIBSC, London, England) was deposited onto freshly cleaved mica´s disks following a previously described procedure.[24] Briefly, mica disks were incubated with APTES 1% ethanol solution for 1 min, washed three times with Milli-Q water and dried with N_2. Afterwards, 50 µl of glutaraldehyde 0.5% water solution were added and incubated for 15 min. After rinsing three times with Milli-Q water, the disks were incubated with purified FHA solution in PBS (10 ng μl^{-1}) for 15 min. Finally the disks were washed with Milli-Q water and were ready to be mounted on the AFM´s liquid chamber.

2.2.ii Cantilever´s tip functionalization

To functionalize the AFM tip we used the glutaraldehyde linking method already published.[24-26] After cleaning the cantilevers with Milli-Q water, 30µl of glutaraldehyde solution (0, 5%) were added to the extreme end of the cantilever, they were incubated during 15 min. and then washed three times with Milli-Q water. Afterwards, the tip was functionalized for 15 min with 30µl of anti-FHA IgG antibody solution (1 ng $\mu l^{-1,}$ NIBSC, London, England) in PBS. Finally, the cantilevers were washed and ready to be mounted in the AFM´s liquid chamber.

2.2.iii AFM measurements and Force Spectroscopy assays

The interactions between the antibody-functionalized tip and purified FHA protein or bacterial cells were performed through force-volume (FV) images using a MultiMode Scanning Probe Microscope (Bruker, Santa Barbara, CA. USA) equipped with a Nanoscope V controller and Nano Wizard III Bioscope (JPK, Berlin, Germany). Each sample was

attached to a steel sample puck (Bruker, Santa Barbara, CA) using a small piece of double side adhesive tape and immediately transferred into the AFM liquid chamber. Two hundred µl of PBS buffer were added to AFM fluid chamber in order to keep the samples hydrated during the course of the experiment. All the measurements were done using contact sharpened silicon nitride probes (NP-10, Bruker) with nominal tip radius of curvature of 20-60 nm. Clean flat muscovite mica surfaces (SPI V-1 grade) were used as rigid substrates for photodetector sensitivity calibration. The spring constants of the cantilevers (K_s) were measured using the thermal tune method and its characteristic values ranged between 0.05 and 0.08 N/m. The surfaces were scanned using the Force Volume (FV) imaging mode at a scan rate of 1 Hz maintaining a maximal applied force of 1nN and 500 ms of surface delay.

Unbinding forces between receptors and ligands depend on the loading rate, i.e. the rate at which the force is applied to the bond. [16, 27-29] To study this issue for our pair FHA-anti-FHA we recorded 1000 Force vs Distance (FD) curves at different retraction velocities (72,100, 500 nm/s) using a 500 nm Z range. The recorded data was analyzed to build the Force vs. ln loading rate curve. After selecting a proper pulling velocity we performed the FV images on living *B. pertussis* Tohama I cells. For these experiments we used a 1000 nm Z range in order to allow the correct detachment of the tip from the sample before starting the next FD curve of the FV array. Two consecutives images were done on single cells, the first image correspond to t=0 and the second to t=40 min since that was the time period separating the acquirement of both images. Ten cells were analyzed from five independent cultures.

The specificity of the interaction events was controlled through blocking experiments. Both, purified FHA on mica and *B. pertussis* Tohama I cells were incubated with a solution of anti-FHA antibody (10 ng μl^{-1}) for 1h before performing the Force Spectroscopy experiments. Another assay was made by performing the Force Spectroscopy measurements on bacterial samples of FHA- strains, which do not express the adhesin on its surface.

2.3. Force-Distance Curve´s Analysis. Determination of Specific Adhesion Events and Young Modulus Calculation

Force vs Distance curve analysis to detect specific adhesion events between the antibody on the tip and either, purified FHA on mica or FHA of the surface envelope of living *B. pertussis* Tohama I cells was done off-line using the OpenFovea software developed by C. Roduit *et al.*[30] Each FD curve was analysed to quantify the magnitude of the force of each specific rupture event and the distance from the point of contact where it occurred. The collected data were represented in the corresponding histograms. Non-specific events

(adhesion peaks without any length separation from the point of contact) were automatically excluded by the software and very low adhesion events (bellow 50 pN) were also excluded as they were considered to be outside the range of antigen-antibodies interactions forces.[16, 31]

In the case of bacterial cells, a nanoindentation analysis was done seeking to discriminate the presence of specific recognition events and rigid domains in the surface. The analysis was done using an in-house developed software, following the procedure described in previous works. [32-34] The zero-force height (z_0; y_0) value of each force curve was manually defined by detecting the point at which the curve begins to lift off from the non-contact baseline when the tip approaches to the sample. [35] After defining the point of contact, Force vs. Distance curves were transformed into Force vs. Indentation depth curves [36], and the resulting data was fitted using a Hertz model for elastic[34, 37] samples and conical indenters. [33 38, 39]

$$F = \frac{2E \tan \alpha}{\pi(1-\nu^2)}\delta^2 \qquad (1)$$

Where F is the loading force, E is the Young modulus, α is the half opening angle of the conical indenter (53°; based in geometrical characteristics of the tip and SEM observations), ν is the Poisson ratio (0,5 for cells [40, 41]) and δ is the indentation.

2.5 Force and Elasticity Maps

FD curves that presented a recognition event on the surface of single bacterium were correlated to their (*x, y)* position on the FV image and plotted as a Force map. The values ranged from 50 to 900 pN and they were represented using a black-white scale. The Young modulus values calculated for *B. pertussis* Tohama I cells were also plotted on surface elasticity maps. Values between 0,15 and 1,1 MPa are depicted in a cyan-blue scale, whereas values between 1,1 and 2 MPa are in a pink-red scale.

2.6 Cluster analysis

From the construction of the force maps, we could define a matrix of forces $F_{ij,}$ with $1 \leq i \leq Lx$, $1 \leq j \leq Ly$, where Lx and Ly represents the number of lines and columns of the force map respectively. In a first step, we made a binarization of the force matrix, defining a threshold value, f_u. In this way, the elements of the binarized matrix can be written as:

$$B_{ij} = 1 \text{ if } F_{ij} \geq f_u$$

$$B_{ij} = 0 \text{ in the opposite case}$$

When the images are built from the binarized matrix, they generate force maps of two

colours. Conventionally, we could interpret each site (i, j) as "occupied" (if B_{ij} =1) or "non-occupied" (if B_{ij} =0). Each site, generically designed by their indexes (i, j), has in the rectangular bidimensional grid four "first neighbours" sites (whose indexes are: (i±1,j), (i,j±1)) and "second neighbours" (whose indexes are: (i+ 1, j + 1), (i +1, j-1), (i-1, j+1), (i-1, j-1)). We will denote $C^{(1)}_{ij}$ and $C^{(2)}_{ij}$ to the numbers of coordination to first and second neighbours of each site respectively, which are interpreted as the number of neighbours occupied without including (in the case of $C^{(1)}_{ij}$) and including (in the case of $C^{(2)}_{ij}$) second neighbours. Both quantities give us a measure of the "agglutination" of the sites, in the sense that when these coordinates are bigger, there would be more connections between the occupied sites.

Another alternative for the statistical characterization of the distribution of the occupied sites can be done by studying the formation of "conglomerates" or "clusters": two occupied sites belong to a same cluster if they can be joined together (admitting diagonal movements and including connections to second neighbours) through occupied sites. On the contrary, if one has to cross at least one non-occupied site, to join two occupied sites, it is assumed that such sites belong to different clusters. Clearly, when the affinity between occupied sites is bigger, the distribution of clusters will tend to acquire a configuration with a relatively small number of clusters and, considering a fixed number of occupied sites in the grid, such clusters will have a relatively important size. When the affinity between sites is low (there is no preference for contact between the sites), clusters will have a smaller size.

3. Results and Discussion

3.1. Force-Distance Curves Analysis

An AFM cantilever´s tip functionalized with a specific antibody as indicated in Material and Methods was used to recognize the presence of FHA adhesin on the surface of live *B. pertussis* cells through Force Spectroscopy assays. Force vs. Z-piezo retraction curves shown in Figure 1 are representative of more than 6000 curves acquired in the above mentioned experiments. During the analysis, the non-specific interactions were automatically excluded by the software by discarding events that did not show any length separation with the contact point.[42] Most of the recorded FD curves showed no adhesion events (Figure 1.a), and are associated to surface areas with no expression of FHA. Other typical FD curves showed one adhesion peak, like the one depicted in Figure 1.b, that exhibits an adhesion event with a magnitude of 130 pN, characteristic for an antigen-antibody interaction.[26, 43] A fewer number of FD curves presented two events occurring at different tip-sample

separations (Figure 1.c). In this case the absolute value of the adhesion force (F_{adh}) was the double of the value (300 pN) detected for most probable single antigen-antibody interaction. This behavior is likely to evidence the interaction of two antigen-antibody pairs at the same time. It is important to remark that during the functionalization of the tip is not possible to guarantee that only one antibody was attached to the tip of the cantilever. In this context when more than one antibody interacts at the same time with proteins in the surface, the magnitude of the interaction peak in the FD curve is typically a multiple of the single interaction force.[26, 28] Other type of FD curves found in our experiments exhibited multiple FHA-antibody interaction events, like the curve represented in Figure 1d that shows three adhesion events that could be understood as three antibodies interacting with three epitopes of the same FHA protein or interacting within neighboring FHA molecules in the underlying surface. Taking a closer look into the last FD curve (Figure 1.d), it is possible to observe a "plateau" that is associated with a different type of interaction, a "tether"- like rupture event. [44] Such adhesion events were frequently observed in our experiments (10-15 %) and can be related to the stretching of a portion of the extracellular membrane as was previously described. [31] When the tip is being pulled off from the surface, in some cases, it makes the external membrane to detach from the structures that maintain it stuck to the cell wall, generating a nanotube of external membrane. When the nanotube is disengaged from the tip a tether rupture event occurs. In the case of Gram-negative bacteria, like *B. pertussis,* the membrane is attached to a thin layer of peptidoglycan present in the intermembrane space through an anchorage lipoprotein. [45]

To check the specificity of the interactions between the antibodies and FHA proteins on the surface, we conducted a Force Spectroscopy assay using the antibody-functionalized tip against purified FHA on mica. As it is known from previous studies, the adhesion force increases with the logarithm of the loading rate in most receptor-ligand bonds.[31] Therefore, we decided to analyze the adhesion events between anti-FHA and the purified protein on mica at three different retracting velocities. A linear relation was obtained between the mean rupture forces and the logarithm of the loading rate as is shown in Figure S1.a along with the corresponding force histogram for the retraction velocity of 500 nm s^{-1} (see Figure S1.b). The most probable adhesion value corresponds to 150 pN, typical for these antigen-antibody interactions. The specificity was determined by incubating the sample with a solution of the antibody before making the Force Spectroscopy experiments under these experimental conditions. The total amount of adhesion events diminished in more than a half (Figure S1.c), although the mean value did not change. This control experiment strongly suggests that the

interaction events between the anti-FHA antibodies and FHA proteins are not artifacts and correspond to specific interactions.

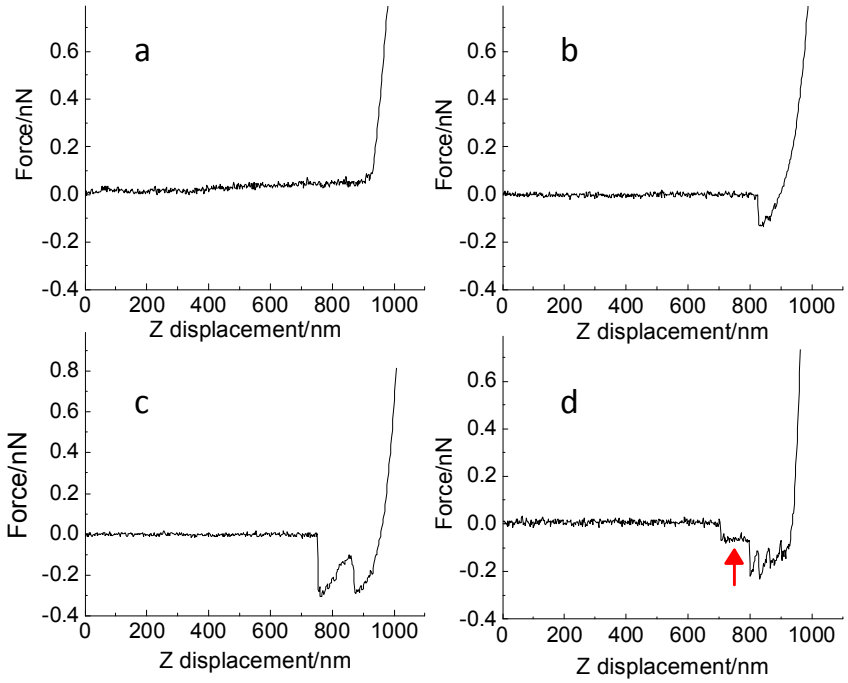

Figure 1. *Representative Force vs Z-piezo displacement measured with an anti-FHA functionalized tip on B. pertussis Tohama I cells supported on glass. a) nonspecific tip-sample interactions, b) one adhesion event, c) two adhesion events in the same FD curve that doubles the typical* F_{adh} *and d), a FD curve with three specific antibody-antigen interactions at different distances followed by a latter "tether" event (pointed by the red arrow) characteristic of the dissociation of a membrane nanotube generated during the retraction of the cantilever.*

3.2 Specific Adhesion Events on the Surface of B. pertussis Cells through Molecular Recognition Experiments

As it was mentioned in section 2.2.iii, two consecutives FV images were recorded on the surface of single *B. pertussis* Tohama I cells with 40 min time lapse between each of them. These studies allowed us to determine the amount as well the magnitude of the recognition events between the antibodies adhered to the tip and the protein FHA in *B. pertussis´* surface. The histograms shown in Figure 2.a and b, represent the adhesion forces detected on 12 individual cells for time = 0 (first scan) and time = 40 min (second scan on the

same cells). In both cases, a great number of retraction curves did not show any adhesion event, representing areas on bacterial surface where there is no expression of the adhesin FHA. For the specific recognition events, the distributions of the histograms are very similar. They include a range of adhesion values from 50 pN to 900 pN, although the majority of the events correspond to low values of interaction forces. In both cases the most probable values correspond to 150 pN, which is a typical interaction value for antigen - antibody pairs as has been previously reported [2, 46, 47] and the most probable value found for the interaction between anti-FHA antibodies and purified FHA mentioned above. Nevertheless, it was possible to differentiate in both histograms, local maximums around values such as 225 and 300 pN. These subpopulations could be associated to the rupture events between two antibodies and one or more proteins in the surface at the same time, which would throw an adhesion value corresponding to the double of the individual rupture event or to the interaction of one antibody plus a Fab fragment of another antibody as it was reported by Hinterdorfer *et al.*[43] The histograms of recognition events on cells have a different distribution of that observed in the Force Spectroscopy experiments for purified FHA-anti-FHA (Figure S1.b) which shows most of the interaction events at low forces. This could be attributed to the soft nature of the cell´s envelope allowing the indentation of the tip which increases the probability of interaction of adhesins with the functionalized tip. This phenomenon would not be feasible to occur in the case of a flat layer of protein deposited onto a hard mica surface. Another parameter calculated from the FD curves was the distance at which the rupture events occurred. These data are represented in Figure 2.c and d for the two studied times. Once again, the distribution of the two populations is the same, meaning that there was no tip contamination during experiments, which would have led to different lengths in the rupture events. Both histograms, for time 0 and time 40 min could be fitted using a LogNormal function; and differently than what occur for purified FHA-anti-FHA interactions, which showed distances with most probable values around 25-50 nm and highest values not further than 25-300 nm, the distances distributions for anti-FHA-Bp Tohama I interactions showed a most probable distance value between 120-160 nm (Fig. 2.c). These values are a bit higher than those expected considering that the length of the non-elongated FHA protein is 50 nm[48] and the length of an antibody is 20 nm.[49] Nevertheless it has to be considered that when the rupture of the interaction occurs, depending on the position of the recognition site, the molecule could be partially or totally extended. It has been reported that the FHA60 fraction (60 kDa N terminal of native FHA) exhibit a 256 nm extension under

force induced elongation.[50] Thus, in our experiments, the typical rupture lengths (120-160 nm) data indicate that the protein is moderately extended. Moreover, the histogram´s values rise up to 800-1000 nm, which represent not only the stretching of the protein but the stretching of the cell's membrane during the cantilever´s retraction.

An important feature to notice is that after 40 min (in the second scan), the total amount of recognition events increased from 1013 to 1274, indicating an increase in the number of affinity sites detected during the second trial. In order to test the specificity of the recognition events, Force distance curves were recorded after exposing *B. pertussis* cells to the same solution of specific antibodies. As a result Force Spectroscopy measurements presented a drastic reduction in the recognition events number (Figure S2.a). This phenomenon can be interpreted as a demonstration of the existence of specific ligand-receptor interactions. Moreover, we made a Force Spectroscopy assay on mutant cells not expressing FHA observing only a few adhesion events whose distribution lacks a well-defined maximum. The observed interactions could represent unspecific events between the antibody and chemical structures on the surface of a cell, probably being of electrostatic nature (Figure S2.b).

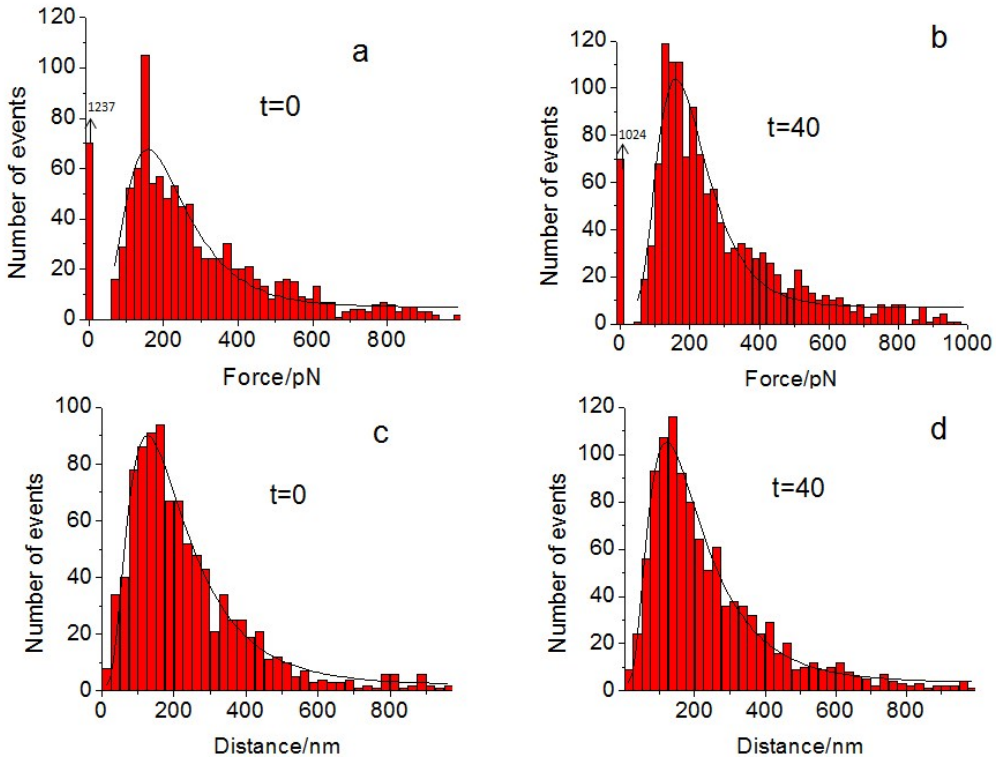

Figure2. *a-b) Adhesion force histograms of the interaction of an anti-FHA functionalized tip and FHA present on the surface of 12 cells of B. pertussis Tohama I at time=0 and time=40 min. All curves were obtained using a retraction speed of 500 nm* s^{-1} *and a surface delay time of 500 ms. Figures c and d represents the distance histogram at which the rupture events plotted in the force histograms occurred for the two times studied.*

3.3 Dynamics of Recognition Events on Individual Bacterium. Force and Elasticity Maps

To evaluate if the increase in the number of found recognition events was representative of each individual studied cell we constructed independent force histograms for each bacterium for 12 cells from 6 independent cultures. Figure 3.a shows a representative FV image of three cells of *B. pertussis* Tohama I strain with their associated force histograms (Figure 3.b). The data on the force histograms can be divided into two subpopulations, in the case of cell *ii* it is possible to detect a first distribution around 200 pN and a second one around 400 pN, whereas cells *i* and *iii*, present a first population around 150 pN and a second one around 300 pN. The most probable values for each distribution are multiple values between them, and are in agreement with the behavior depicted by the overall data described in section 3.2. In every individual cell, the amount of specific recognition events rose between the first and the second scans, in cell *i* the percentage increased from 49% to 73%, in

cell *ii* from 40 to 48% and in cell *iii* from 50 to 71% suggesting that the general behavior observed for the whole population of studied cells (section 3.2) is representative of the individual performance of the cells. Moreover, the other 9 analyzed cells also showed an increase in the recognition events from 8 to 28% after 40 minutes (see Table S1 and Fig S6 and S7 in Supp information).

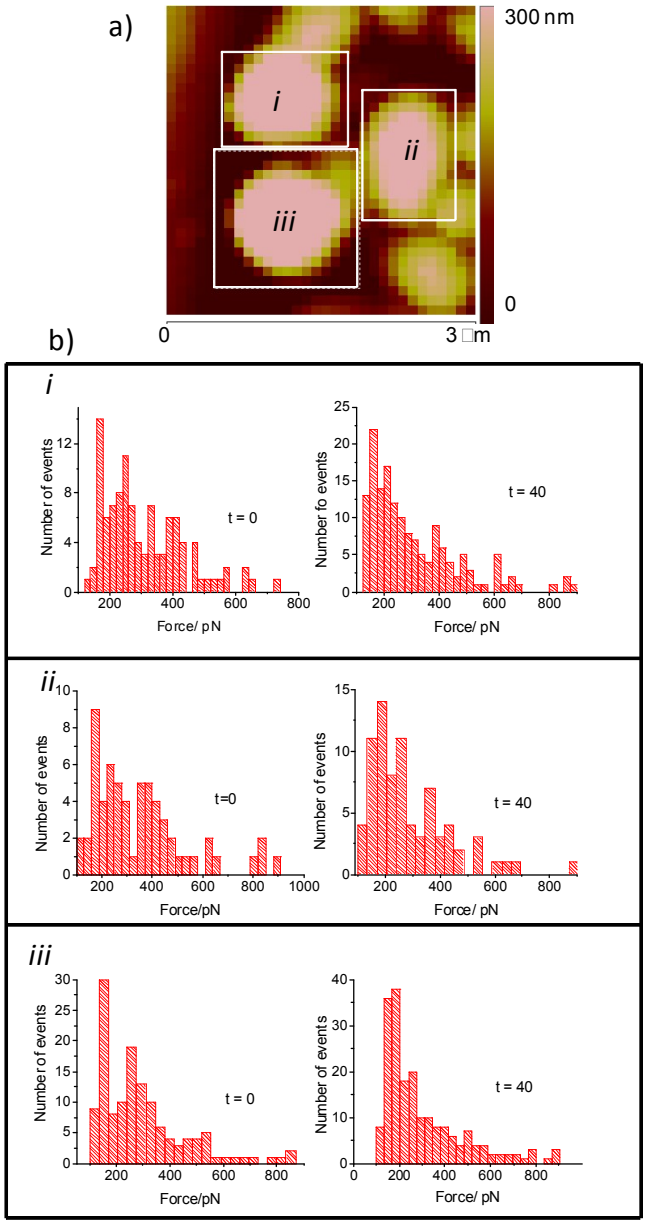

Figure 3-*a) Force Volume image of three individual B. pertussis Tohama I cells acquired with a functionalized tip. b) The specific recognition events between FHA-antiFHA on the surface of cells shown in a) are represented in the corresponding histograms for the respective time points studies (0 and 40 min). In every case the number of adhesion events rose in the second FV image.*

To elucidate if the new recognition events on the surface of the cells are distributed randomly or if they are organized in any special arrangement we decided to build the associated force maps by correlating the FD curves with their (*x, y)* coordinates on the corresponding FV image (Figure 4). It is possible to observe that in every case the amount of non-null force pixels is higher in the second scan (40 min) compared to the first one (t=0) although it is not possible to define if they are being organized in any specific way. Nevertheless, one particular area (inside the red circle in Figure 4a) on bacterium *iii* drew our attention. It corresponds to a cell to cell contact area and it has, clearly, more recognition events clustering in the zone after the second scan with the functionalized tip (Figure 4.b,c). Surprisingly, the neighbour cell (*ii*) also showed a clustering or adhesion events in the contact area after 40 min, like is shown in Figure S3. This result is very interesting since FHA is the major adhesin of *B. pertussis*, responsible not only for the initial attachment to human cells, but also as an important element of bacterium-bacterium interactions involved in the auto agglutinogen capacity and microcolony formation. [5] An enhancement in the number of FHA binding sites in the contact area between two cells would be indicating a stimulus for cell to cell interactions. Taking into account that previously published results from our group suggested that nanodomains of FHA on the surface of *B. pertussis* correlates with more rigid areas in the envelope[36], we decided to evaluate the Young modulus for this particular bacterium and plotted it as an elasticity map of the surface. In Figure 4.d, e is possible to observe the corresponding maps were the soft values are represented in a blue-cyan scale and the stiffer values are represented in a pink-red scale. The circled area (red line) represents the contact area between the two cells, and it is clearly observable that the elasticity of the envelope rises from soft to rigid values in the second scan, accompanying the increase of recognition events in the same area.

The absolute values of Young modulus calculated from the approach curves in the present analysis are much higher (up to 2 MPa) than the values obtained from our previous report, where the maximum value was 1 MPa.[36] This issue can be explained taking into account the difference in the Z range of the FD curves in each experiment. In the current assays, the Z range was 1 μm in order to allow a correct detachment of the interacting molecules in the tip and the surface. This Z range, even though needed for these experiments, represents a compromise situation for selecting correctly the nonlinear zone of the approach curve to be fitted with the Hertz´s model. In this sense, part of the linear behavior of the curves is being incorporated to the nonlinear fit, resulting in enhanced Young modulus values. Nevertheless, as this effect existed in every studied curve, the calculated E values can

be compared in a relative manner.

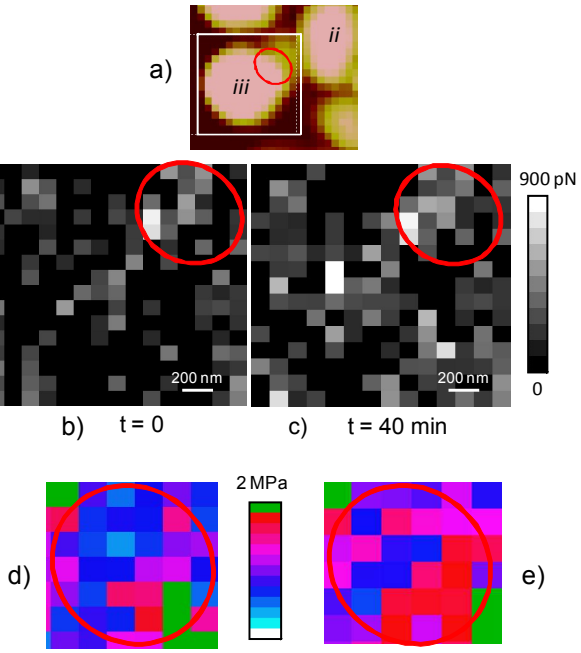

Figure 4- *a) The circled area (red line) represents the contact zone between two bacteria (iii and ii in Figure 3a), where it is possible to observe an increase in the recognition events after 40 min (b and c). The same contact area in the elasticity maps (d and e) is circled by red lines. The envelope changes from soft to rigid values in the second scan (e) accompanying the raise in the recognition events for the domain as shown in b-c.*

3.4 Cluster and Nearest Neighbor's Analysis

To clarify if the new events that appeared in the cells after 40 min of scanning the surface with a functionalized tip are arranged in any particular manner we decided to perform a cluster analysis using the data from the force maps. The null events were assigned to non-cluster pixels, and each of the positive values of interaction forces in the maps were assigned to a single cluster on the surface. Bigger clusters were defined from single no null values connected between them through lateral and diagonal contacts. The results indicate that in every case, the amount of clusters diminished from the first to the second force map but the size of connected clusters markedly increases. In the case of cell *i* in Figure 3, the clusters were reduced to the half (16 to 8), cell *ii* showed a change from 10 to 7 clusters after 40 min and cell iii exposed the most important reduction in the clusters that went from 14 to only 3 larger clusters in the second FV (Figure 5 and Figures S4 and S5 in Supp.Inf.). We have also calculated the mean number of first and second nearest neighbors for each non-null force

value which in every case increases from the first to the second scan. These results indicate that consecutive scans of a *B. pertussis* Tohama I bacterium with a specific antibody against FHA, increase the binding sites of FHA protein on the surface of the cell and generates, probably along with the existing nanodomains, bigger areas of clustered adhesins.

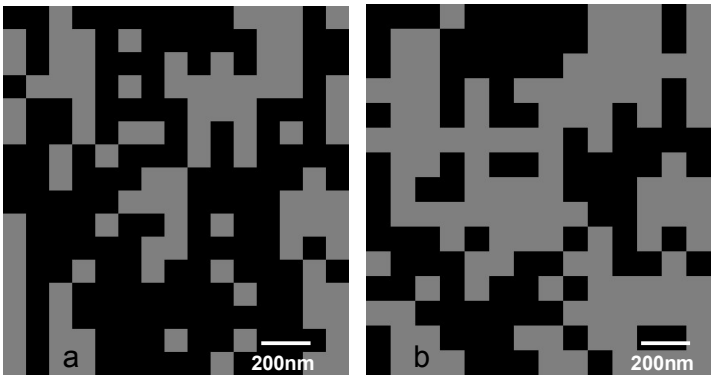

Figure 5: *Cluster analysis for cell iii in Figure 3.a .a) t= 0. Recognition events (grey) = 95. Clusters=14. Average coordination number: First neighbors=1.23, second neighbors=2.28. b) t= 40 min. Recognition events = 116. Clusters = 3. Average coordination number: first neighbors=1.94, second neighbors=3.78. Non-recognition events in black.*

The above results for individual cells were obtained for 12 cells from 6 independent cultures. Increments ranging 8-28% were obtained for the recognition events accompanied by a decrease in the number of clusters (see Table S1 in Supp. Inf. and two representative cells in Figures S6 and S7)

In light of these results the question arises about the reason for the rearrangement of protein in the cell′s surface. One possibility, as was mentioned before, is that the chemical, specific interaction between the protein and the antibody on the AFM tip induces the recruitment of more FHA and its reorganization. Another interpretation could be that the mechanical pressure exerted during the continuous scanning of the envelope could trigger the mobilization of the adhesins non-exposed in the surface during the first scan. To answer the latter option we have made two consecutives Force Volume images on a single bacterium using a non-functionalized tip and we analyzed the behavior of the Young modulus in order to determine the organization of rigid nanodomains after 40 min. The results indicated no changes in the rigid domains between the two scans (Figure S8) leading us to think that the mechanical stimulus is not responsible for the rearrangement of FHA. Discarding the nonspecific pressure made by the tip we focus in the discussion of whether the consecutive

scanning with the functionalized tip could stimulate the synthesis and exposition of more FHA proteins and/ or adhesin diffusion from non-scanned parts of the bacterial surface or if the increase in recognition events is a consequence of conformational changes induced by the specific applied force. To answer these questions we performed several Force Spectroscopy assays on individual heat-inactivated bacterium. The results shown in Table 1 indicate that even in killed bacteria there is an increase of recognition events after 40 min along with a reduction in the number of clusters that indicates a rearrangement of the exposed proteins into domains as was observed in live cells. This phenomenon would not involve synthesis or diffusion of FHA that, up to our knowledge, in bacterial metabolism are energy-dependent processes.[51] We propose that the specific force induced to which FHA proteins are subjected during the experiments could trigger conformational changes in the protein leading to the exposure of homo-recognition sites (probably exposure of tandem repeats) allowing an initial FHA-FHA interaction that latter recruits more neighboring adhesins. These interactions could be possibly due to the length of native FHA (50 nm) which confers rotational mobility to the macromolecules like it was suggested for Als proteins in yeasts. [18] Also in line with our results Lecuyer *et al.* [52] reported that mechanical stress could lead to a physical deformation or a biological (chemical surface modification, higher density of binding sites) response of bacteria, resulting in an increased number of bonds created between the cell and the surface. In the same context, Thomas et al. have reported that shear forces induce conformational changes in adhesins that result in a shear-dependent binding.[53]

Table 1

Recognition events and clusters evolution in heat-killed cells

	% Increase in recognition events after 40 min	Clusters a t= 0 min	Clusters a t=40 min
Cell I	15	22	6
Cell II	23	5	1
Cell III	12	9	8

As it was mentioned before, FHA is the most abundant adhesin of *B. pertussis*. FHA has at least three recognition domains to attach to the host´s tissue cells. It mediates the adhesion to epithelial cells through the recognition of heparan-sulfates molecules present in the extracellular matrix and also mediates the adhesion to macrophages and non-ciliated

epithelial cells.[11] We propose, based in our experimental results, that the specific recognition between FHA and chemical groups in the surface of the host´s cells under shear mechanical stress originates stretching forces in the protein that could trigger the recruitment of other adhesins molecules, clustering them into the focal contact site to enhance the interaction.

To our knowledge this is the first time that a rearrangement of adhesins is followed at the molecular level on the surface of single live bacterium, and it represents an important contribution to understand the significance of its nanodomains clustering on the surface of the cells. This mechanism would be a fast and effective manner to interact with the host´s tissues favoring the first adhesion step, which constitutes a universally important stage in the establishment of an infection. The shear-enhanced adhesion could contribute to the way employed by *B. pertussis* to colonize surfaces under turbulent conditions.

Conclusions

The results reported in this work demonstrated a force induced clustering of an important adhesin of *Bordetella pertussis* like FHA occurring when specific molecular recognition events take place. The force induced reorganization of the adhesin in the surface of the cells could explain a reinforced adhesive response under external forces which could be determinant in the very first adhesion events mediated by the interaction of this protein with the host´s tissue cells. This single-molecule information contributes to the understanding of basic molecular mechanisms used by bacterial pathogens to cause infectious disease and to gain insight into the structural features by which adhesins can act as force sensors under mechanical shear conditions.

Acknowledgments: We acknowledge support from ANPCyT (Argentina, PICT-2010-2554, PICT-2012-1808, PICT-2012-2514), CONICET (Argentina, PIP 11220090100139), and from Dirección de Relaciones Internacionales-MINCYT-Argentina. LA and NC are fellows from CONICET. MEV is a member of the research career of CIC, Bs As, Argentina.

References

1. F. R. Mooi, I. H. van Loo and A. J. King, *Emerg Infect Dis*, 2001, **7**, 526-528.
2. W. Hellenbrand, D. Beier, E. Jensen, M. Littmann, C. Meyer, H. Oppermann, C. H. Wirsing von Konig and S. Reiter, *BMC Infect Dis*, 2009, **9**, 22.
3. M. S. Conover, G. P. Sloan, C. F. Love, N. Sukumar and R. Deora, *Mol Microbiol*, 2010, **77**, 1439-1455.
4. G. P. Sloan, C. F. Love, N. Sukumar, M. Mishra and R. Deora, *J Bacteriol*, 2007, **189**, 8270-8276.
5. D. O. Serra, M. S. Conover, L. Arnal, G. P. Sloan, M. E. Rodriguez, O. M. Yantorno and R. Deora, *PLoS ONE*, 2011, **6**, e28811.
6. R. M. Donlan and J. W. Costerton, *Clin Microbiol Rev*, 2002, **15**, 167-193.
7. M. S. Conover, G. P. Sloan, C. F. Love, N. Sukumar and R. Deora, *Mol. Microbiol.*, 2010, **77**, 1439-1455.
8. J. A. Melvin, E. V. Scheller, J. F. Miller and P. A. Cotter, *Nat Rev Micro*, 2014, **12**, 274-288.
9. S. M. Prasad, Y. Yin, E. Rodzinski, E. I. Tuomanen and H. R. Masure, *Infect Immun*, 1993, **61**, 2780-2785.
10. F. D. Menozzi, C. Gantiez and C. Locht, *FEMS Microbiol Lett*, 1991, **62**, 59-64.
11. C. Locht, P. Berlin, F. D. Menozzi and G. Renauld†, *Mol. Microbiol.*, 1993, **9**, 653-660.
12. D. Serra, A. Bosch, D. Russo, M. Rodríguez, Á. Zorreguieta, J. Schmitt, D. Naumann and O. Yantorno, *Anal.Bioanal.Chem.*, 2007, **387**, 1759-1767.
13. J. J. Heinisch, V. Dupres, S. Wilk, A. Jendretzki and Y. F. Dufrêne, *PLoS ONE*, 2010, **5**.
14. D. J. Müller and Y. F. Dufrêne, *Current biology : CB*, 2011, **21**, R212-R216.
15. C. Verbelen, D. Raze, F. Dewitte, C. Locht and Y. F. Dufrêne, *J Bacteriol*, 2007, **189**, 8801-8806.

16. Y. F. Dufrêne, D. Martinez-Martin, I. Medalsy, D. Alsteens and D. J. Muller, *Nat Methods*, 2013, **10**, 847-854.
17. P. Tripathi, A. Beaussart, G. Andre, T. Rolain, S. Lebeer, J. Vanderleyden, P. Hols and Y. F. Dufrêne, *Micron*, 2012, **43**, 1323-1330.
18. D. Alsteens, M. C. Garcia, P. N. Lipke and Y. F. Dufrêne, *PNAS*, 2010, **107**, 20744-20749.
19. P. N. Lipke, M. C. Garcia, D. Alsteens, C. B. Ramsook, S. A. Klotz and Y. F. Dufrêne, *TrendsMicrobiol.*, 2012, **20**, 59-65.
20. S. El-Kirat-Chatel, A. Beaussart, C. D. Boyd, G. A. O'Toole and Y. F. Dufrêne, *ACS Chem Biol*, 2014, **9**, 485-494.
21. C. Locht, M. C. Geoffroy and G. Renauld, *EMBO J.*, 1992, **11**, 3175-3183.
22. G. A. Burks, S. B. Velegol, E. Paramonova, B. E. Lindenmuth, J. D. Feick and B. E. Logan, *Langmuir*, 2003, **19**, 2366-2371.
23. V. Vadillo-Rodríguez, H. J. Busscher, W. Norde, J. de Vries, R. J. B. Dijkstra, I. Stokroos and H. C. van der Mei, *Appl. Environ. Microbiol.*, 2004, **70**, 5441-5446.
24. A. Yersin, H. Hirling, P. Steiner, S. Magnin, R. Regazzi, B. Huni, P. Huguenot, P. De los Rios, G. Dietler, S. Catsicas and S. Kasas, *Proc Natl Acad Sci U S A*, 2003, **100**, 8736-8741.
25. P. Steiner, S. Alberi, K. Kulangara, A. Yersin, J. C. Sarria, E. Regulier, S. Kasas, G. Dietler, D. Müller, S. Catsicas and H. Hirling, *EMBO J*, 2005, **24**, 2873-2884.
26. C. Roduit, F. G. van der Goot, P. De Los Rios, A. Yersin, P. Steiner, G. Dietler, S. Catsicas, F. Lafont and S. Kasas, *Biophys J*, 2008, **94**, 1521-1532.
27. T. Strunz, K. Oroszlan, I. Schumakovitch, H. Guntherodt and M. Hegner, *Biophys J*, 2000, **79**, 1206-1212.
28. V. Dupres, F. D. Menozzi, C. Locht, B. H. Clare, N. L. Abbott, S. Cuenot, C. Bompard,

D. Raze and Y. F. Dufrêne, *Nat Meth*, 2005, **2**, 515-520.

29. B. Bonanni, A. S. Kamruzzahan, A. R. Bizzarri, C. Rankl, H. J. Gruber, P. Hinterdorfer and S. Cannistraro, *Biophys J*, 2005, **89**, 2783-2791.
30. C. Roduit, B. Saha, L. Alonso-Sarduy, A. Volterra, G. Dietler and S. Kasas, *Nat Methods*, 2012, **9**, 774-775.
31. D. J. Müller, J. Helenius, D. Alsteens and Y. F. Dufrêne, *Nat Chem Biol*, 2009, **5**, 383-390.
32. M. Radmacher, J. P. Cleveland, M. Fritz, H. G. Hansma and P. K. Hansma, *Biophys. J.*, 1994, **66**, 2159-2165.
33. A. Touhami, B. Nysten and Y. F. Dufrêne, *Langmuir*, 2003, **19**, 4539-4543.
34. P. Polyakov, C. Soussen, J. Duan, J. F. L. Duval, D. Brie and G. Francius, *PLoS ONE*, 2011, **6**, e18887.
35. F. Gaboriaud and Y. F. Dufrêne, *Colloids Surf., B*, 2007, **54**, 10-19.
36. L. Arnal, D. O. Serra, N. Cattelan, M. F. Castez, L. Vazquez, R. C. Salvarezza, O. M. Yantorno and M. E. Vela, *Langmuir*, 2012, **28**, 7461-7469.
37. M. Arnoldi, M. Fritz, E. Bäuerlein, M. Radmacher, E. Sackmann and A. Boulbitch, *Phys.Rev.E*, 2000, **62**, 1034-1044.
38. F. Gaboriaud, S. Bailet, E. Dague and F. Jorand, *J. Bacteriol.*, 2005, **187**, 3864-3868.
39. S. B. Velegol and B. E. Logan, *Langmuir*, 2002, **18**, 5256-5262.
40. E. A-Hassan, W. F. Heinz, M. D. Antonik, N. P. D Costa, S. Nageswaran, C.-A. Schoenenberger and J. H. Hoh, *Biophys. J.*, 1998, **74**, 1564-1578.
41. P. A. Pinzón-Arango, R. Nagarajan and T. A. Camesano, *Langmuir*, 2010, **26**, 6535-6541.
42. O. H. Willemsen, M. M. Snel, K. O. van der Werf, B. G. de Grooth, J. Greve, P. Hinterdorfer, H. J. Gruber, H. Schindler, Y. van Kooyk and C. G. Figdor, *Biophys J*,

1998, **75**, 2220-2228.

43. P. Hinterdorfer, W. Baumgartner, H. J. Gruber, K. Schilcher and H. Schindler, *Proc Natl Acad Sci U S A*, 1996, **93**, 3477-3481.
44. R. G. R. Arturo M. Baro ed., *Atomic Force Microscopy in Liquid: Biological Applications*, Wiley-VCH Verlag GmbH & Co. KGaA, 2012.
45. N. Kango, *Textbook of Microbiology*, I. K. International Publishing House Pvt. Ltd., New Delhi, 2010.
46. F. Kienberger, G. Kada, H. Mueller and P. Hinterdorfer, *J Mol Biol*, 2005, **347**, 597-606.
47. H. Gao, X. X. Zhang and W. B. Chang, *Front Biosci*, 2005, **10**, 1539-1545.
48. A. V. Kajava, N. Cheng, R. Cleaver, M. Kessel, M. N. Simon, E. Willery, F. Jacob-Dubuisson, C. Locht and A. C. Steven, *Mol. Microbiol.*, 2001, **42**, 279-292.
49. S. Ido, H. Kimiya, K. Kobayashi, H. Kominami, K. Matsushige and H. Yamada, *Nat Mater*, 2014, **13**, 264-270.
50. D. Alsteens, N. Martinez, M. Jamin and F. Jacob-Dubuisson, *PLoS ONE*, 2013, **8**.
51. A. L. Lehninger, D. L. Nelson, M. M. Cox and D. L. Nelson, eds., *Lehninger Principles of Biochemistry*, W H Freeman & Co, Gordonsville, 2004.
52. R. R. Sigolene Lecuyer, Yi Shen, Alison Forsyth, Hera Vlamakis, Roberto Kolter, and Howard A. Stone, *Biophys. J.*, 2011, **100**, 341-350.
53. W. E. Thomas, E. Trintchina, M. Forero, V. Vogel and E. V. Sokurenko, *Cell*, 2002, **109**, 913-923.